The Jahn–Teller effect in the SrLaGa$_3$O$_7$:Co^{2+} system

Marek Grinberg[1], Sławomir M Kaczmarek[2], Marek Berkowski[3] and Taiju Tsuboi[4]

[1] Institute of Experimental Physics, University of Gdańsk, Wita Stwosza 57, 80-952 Gdańsk, Poland
[2] Institute of Optoelectonics, Military University of Technology, 2 Kaliski Street, 00-908 Warsaw, Poland
[3] Institute of Physics, Polish Academy of Sciences, 32/46 Lotników Street, 02-668 Warsaw, Poland
[4] Faculty of Engineering, Kyoto Sangyo University, Kamigamo, Kita-ku, Kyoto 603-8555, Japan

Abstract
We have presented absorption spectra related to octahedrally coordinated Co^{2+} in the Sr^{2+} position in SrLaGa$_3$O$_7$. Quantitative analysis of the line shape of the ^{4}T$_1 \to {}^4$T$_2$ transition shows the existence of the strong T $\otimes$ τ Jahn–Teller effect in the ^{4}T$_1$ ground state of the system. We have estimated the Jahn–Teller stabilization energy to be equal to 507 cm^{-1}. The procedure of estimation of the crystal-field strength parameter $10Dq$ for the system that is affected by the strong Jahn–Teller coupling has been discussed.

1. Introduction

SrLaGa$_3$O$_7$ (SLGO) belongs to the family of binary gallates of alkaline- and rare-earth metals. Crystals of these compounds have the tetragonal gehlenite (Ca$_2$Al$_2$SiO$_7$) structure (space group: $P\bar{4}2_1m_1$, D$_{2d}^3$) with the unit-cell parameters $a = 0.8058$ nm and $c = 0.5333$ nm. Gehlenites such as BaLaGa$_3$O$_7$ (BLGO) [1], SrLaGa$_3$O$_7$ (SLGO) [2, 3] and SrGdGa$_3$O$_7$ (SGGO) have been manufactured as matrix materials for potential laser and display applications. They were doped with neodymium [4], praseodymium [5] and chromium [6]. Although SLGO crystals doped with various rare-earth ions have been investigated extensively [2–5, 7–9], there has been no detailed report on the optical properties of SLGO doped with Co^{2+} ions.

The Co^{2+} ions are expected to substitute for octahedrally coordinated Sr^{2+} ions. The crystal field splits the sevenfold-degenerate ^{4}F state into an orbital triplet ^{4}T$_1$, followed by another orbital triplet ^{4}T$_2$ and an orbital singlet ^{4}A$_2$ [10]. The next higher state of the free Co^{2+} ion yields in a crystal field the ^{4}T$_1$(^{4}P) configuration. The spin–orbit interaction and low-symmetry field split the twelvefold-degenerate ^{4}T$_1$ level into a number of Kramers doublets. Co^{2+} in an octahedral field was investigated in various lattices a long time ago [11]. However, there are still many questions that are not clearly resolved and therefore have to be discussed. These especially concern the electron–lattice interaction, the effect that is responsible for the homogeneous broadening of optical transitions and results in specific absorption band shapes. In the present paper the behaviour of Co ions intentionally introduced into the crystal lattice

is investigated by means of an optical technique. We focus mainly on the Jahn–Teller effect in the ground state of the Co^{2+}.

2. Experimental procedure

2.1. Single-crystal growth of SLGO:Co

Single crystals of $SrLaGa_3O_7$ doped with cobalt (SLGO:Co) have been grown using the Czochralski method in a nitrogen atmosphere and the floating-zone method with optical heating in air. Crystals were pulled from a 40 mm diameter iridium crucible in a nitrogen atmosphere containing 1 vol% of oxygen in the $\langle 001 \rangle$ direction on oriented seed crystals. The pulling rate was decreased over the range from 2.2 mm h^{-1} to 1 mm h^{-1} as the cobalt concentration in the melt was increased. The starting concentrations of Co in the melt were 0.15, 0.3, 2 and 3 mol% with respect to Ga in the Czochralski method, whereas they were 2 and 4 mol% in the floating-zone method. The floating-zone method was employed in order to determine the maximum dopant concentration at which the crystals obtained are still transparent.

High-purity carbonate, $SrCO_3$ (4N5), and the oxides La_2O_3 (5N), Ga_2O_3 (5N) and Co_3O_4 (3N) were used as the starting materials. The starting melt composition was calculated on the basis of the congruent melting composition $Sr_{1.04}La_{0.935}Ga_{3.02}O_{7-\delta}$. The concentrations of cobalt admixture in the starting melts with reference to gallium were equal to 0.15 mol%, 0.3 mol%, 2 mol% and 3 mol%. The crystals obtained have diameter 20 mm and length up to 60 mm. They had a blue colour whose intensity increased with increasing dopant concentration. In the crystals with the highest cobalt concentration, precipitations extending along the crystal growth direction with a diameter of around 1 mm appeared in the core region. Since the crystal obtained by the floating-zone method from the melt containing 4 mol% of Co was non-transparent, we decided to limit the dopant concentration for the Czochralski method to 3 mol.%.

2.2. Absorption measurements

To study the optical properties of the SLGO:Co single crystals, polished on both sides, parallel-plate samples of thickness from 0.3 to 1 mm were prepared. The absorption spectra were taken at 300 K in the spectral range between 190 and 25 000 nm using LAMBDA-900 Perkin-Elmer and FTIR 1725 Perkin-Elmer spectrophotometers. Although it was searched for, the emission related to Co^{2+} in the visible and near-infrared region was not observed. In this paper, we present the absorption spectra of a crystal containing Co at 3 mol% concentration.

3. Results and discussion

The absorption line shape of the $SrLaGa_3O_7$:Co is presented in figure 1(a). The line shape was obtained from the absorption spectrum by dividing the absorption by the photon energy [12]. The main features of the spectrum consist of a double band in the IR region (5000–7500 cm^{-1}) and a triple band in the visible region (12 500–20 000 cm^{-1}). The latter absorption band is responsible for the blue colour of the sample. We have noticed also strong absorption in the far IR, and in the UV region (not indicated in the figure).

One can analyse the spectrum of Co^{2+} (an octahedrally coordinated $3d^7$ system) using the crystal-field approach [12, 13], which yields the energetic structure of the ion in the form of a Tanabe–Sugano diagram determined by the crystal-field strength parameter $10Dq$, the Racah
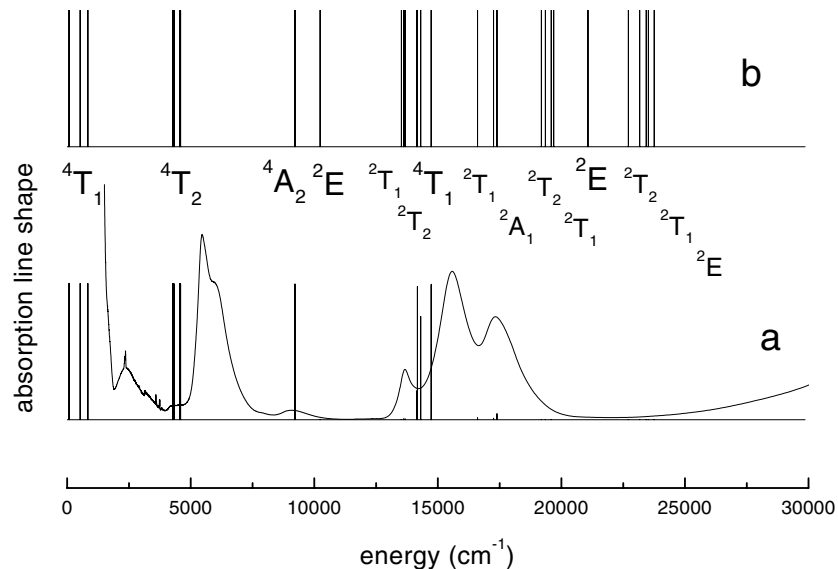
Figure 1. (a) The absorption spectrum of SrLaGa$_3$O$_7$:Co^{2+} (solid curve); the vertical lines represent the percentages of the quartet in the respective states. (b) Energies of the Co^{2+} calculated in the framework of the crystal-field approach (see the text).

parameters B and C, and the spin–orbit coupling ζ. In figure 1(b) we present the energetic structure of the octahedrally coordinated Co^{2+}, which was calculated for $10Dq = 4750$ cm^{-1}, $B = 720$ cm^{-1}, $C = 3170$ cm^{-1} and spin–orbit coupling constant $\zeta = 400$ cm^{-1}. Although we have obtained a relatively small value of $10Dq$, the values of the other parameters obtained here are still quite close to the data obtained by Ferguson *et al* [11] for Co^{2+} in CoBr$_2$, KCoF$_3$, CoCl$_2$ and CoWO$_4$ ($10Dq = 6400$–8000 cm^{-1}, $B = 760$–880 cm^{-1}, $C = 4.4B$ and $\zeta = 400$–500 cm^{-1}), and by Tsuboi and Iio for Co^{2+} in CsCoBr$_3$ [14] ($10Dq = 6400$ cm^{-1}, $B = 760$ cm^{-1}, $C = 4.4B$ and $\zeta = 420$ cm^{-1}). It seems that the values of the parameters that we have used reproduce the energy of the $^4T_1 \rightarrow {}^4A_2$ absorption band. On the other hand, one can see that the calculated energy of the $^4T_2$ multiplet results in an energy for the $^4T_1 \rightarrow {}^4T_2$ absorption band that is smaller than that detected experimentally. The situation is similar for the $^4T_1 \rightarrow {}^4T_1$ transition. Such a deviation is attributed to the strong Jahn–Teller coupling of the ground state. For such a system, the real crystal-field strength $10Dq$ is much smaller than the energy of the absorption band, as will be discussed later.

One notices that the ground state of the system is a well defined spin–orbit- and Jahn–Teller-split $^4T_1$ multiplet. Considering the relative intensities of the absorption bands, our spectra are consistent with the spin-selection rule that allows only quartet–quartet transitions and forbids transitions from the ground state to the excited doublets. Ferguson *et al* [11] have noticed a similar effect. In the case of Co^{2+} in CoBr$_2$KCoF$_3$, KMg(Co)F$_3$, CoCl$_2$ and CoWO$_4$, they have obtained an absorption related to transitions from the $^4T_1$ ground state to the excited quartet states stronger than that related to the transitions from the ground state to the excited doublet states. In the case of CsCoBr$_3$ [14] it was found that the spin-selection rule is not so strictly obeyed, since transitions to doublets and quartets give comparable absorption. Assuming that the spin-selection rule works in the case of SrLaGa$_3$O$_7$:Co^{2+}, we have considered that the absorption coefficient has to be proportional to the percentage of the quartet in the respective excited state.

To obtain the wave function, we have considered the standard Tanabe–Sugano Hamiltonian [13], which includes the spin–orbit interaction. In this way, one obtains the wave function of the excited electronic manifold, given by the following formula:

$$\phi_v = \sum_l a_{vl}(s_l = 1/2)\varphi_l + \sum_m a_{vm}(s_m = 3/2)\varphi_m. \tag{1}$$

Since the ground state is the quartet ($s = 3/2$), the probability of the absorption to the v-electronic manifold is given by

$$P_{gv} = \sum_m |a_{vm}(s_m = 3/2)|^2. \tag{2}$$

In figure 1(a) the heights of the solid vertical lines are proportional to the percentages of the quartet in the given state. It is seen that one can reproduce the transitions from the ground state to the $^4T_2$ and $^4T_1$ states. Also, the strength and position of the spin-allowed $^4T_1 \rightarrow {}^4A_2$ transition seem to be well fitted.

We will now consider the phenomena that could be responsible for the structure of the absorption. If it is spin–orbit coupling of the first excited $^4T_2$ state or the splitting of this state by the static low-symmetry field, one expects absorption consisting of the superposition of bands of comparable halfwidth. Since this is not the case here, we prefer to interpret the structure of the absorption in the framework of the static strong Jahn–Teller effect. Actually, since we are dealing with two very smooth broad bands without any internal structure, the assumed spin–orbit coupling equal to 400 cm^{-1} is rather overestimated.

The triple structure between 12 500 cm^{-1} and 20 000 cm^{-1} is quite far from the recovered position of the mixed states: the $^4T_1$ quartet and $^2T_1$, $^2T_2$, $^2T_1$ and $^2A_1$ doublets for an assumed spin–orbit coupling of 400 cm^{-1}. To get a better fit, one has to consider the unreliable value of the spin–orbit interaction, equal to a few thousand wavenumbers. Therefore, in this case also, the splitting can be related to the large static Jahn–Teller effect.

We have analysed in a more detailed way the structure of the absorption band related to the $^4T_1 \rightarrow {}^4T_2$ transition. This feature consists of two bands. The narrower band (indicated as 1, hereafter) is peaked at about 5450 cm^{-1}, whereas the broader band (indicated as 2) is peaked at 6050 cm^{-1}. When one interprets these bands as homogeneously broadened, it is easily seen that each has a zero-phonon line (although these lines are not seen) at an energy approximately equal to 5000 cm^{-1}. To analyse the spectrum line shape, we have assumed that the $^4T_1$ ground state and the $^4T_2$ excited states are split by the Jahn–Teller effect. We have considered coupling to the two-dimensional ε-mode and three-dimensional τ-mode separately.

In the case of $T \otimes \varepsilon$ coupling, lattice vibrations take place in the two-dimensional configurational space $\{Q_\theta, Q_\varepsilon\}$. The adiabatic energy surfaces of the ground and excited electronic manifolds are given by the following Hamiltonian [15, 16]:

$$\frac{1}{2}Q_\theta^2 + \frac{1}{2}Q_\varepsilon^2 + V^{e,g}\begin{bmatrix} Q_\theta - \sqrt{3}Q_\varepsilon & 0 & 0 \\ 0 & Q_\theta + \sqrt{3}Q_\varepsilon & 0 \\ 0 & 0 & -2Q_\theta \end{bmatrix} \tag{3}$$

where superscripts 'e' and 'g' correspond to the excited state and ground state, respectively. Each of the two states, the ground $^4T_1$ and the excited $^4T_2$, splits into three equivalent electronic manifolds that define the vibronic potentials represented by two-dimensional paraboloids with minima at

$$\bar{Q}_1^{ge} = -V^{ge}(\bar{q}_\theta - \sqrt{3}\bar{q}_\varepsilon)$$
$$\bar{Q}_2^{ge} = -V^{ge}(\bar{q}_\theta + \sqrt{3}\bar{q}_\varepsilon) \tag{4}$$
$$\bar{Q}_3^{ge} = 2V^{ge}\bar{q}_\theta.$$

Here $\bar{q}_\varepsilon$ and $\bar{q}_\theta$ are unit vectors in the respective directions. The positions of the minima of the energy for the ground and excited manifolds are presented in figure 2(b). According to relation (4), the Jahn–Teller stabilization energies in the ground and excited states are given by

$$E_{JT(T\otimes\varepsilon)}^{g,e} = -2(V^{g,e})^2. \tag{5}$$

In general, the symmetry allows one to consider two independent vibration modes that are parallel and perpendicular to the Jahn–Teller displacements for each electronic manifold. Thus the model that we have used assumes that the potential energy surfaces of the individual electronic manifolds are given by the following relation:

$$U(Q) = \hbar\omega_\parallel \frac{1}{2}(Q_\parallel - Q_\parallel^0)^2 + \hbar\omega_\perp \frac{1}{2}Q_\perp^2 \tag{6}$$

where subscripts $\parallel$ and $\perp$ correspond to the vibration parallel and perpendicular to the Jahn–Teller displacement. Here $Q_\parallel^0 = q_0$ and $Q_\parallel^0 = q_1$ for the ground and excited state, respectively. The displacement corresponding to the minimum energy of the perpendicular vibrations is always zero. An example of an equipotential surface (for $Q_\parallel$ parallel to the ε-axis) is presented in figure 2(b). To obtain good correspondence between the theoretically calculated and experimental absorption line shapes, we have to assume that the Jahn–Teller effect in the ground state is much stronger. Considering the Frank–Condon rule, one can see that the transitions that start from the individual minima of the ground electronic manifold form two bands peaked at the energies (see figure 2(b))

$$E_1 = E_0 + \frac{1}{2}\{\Delta_1\}^2$$
$$E_2 = E_0 + \frac{1}{2}\{\Delta_2\}^2 \tag{7}$$
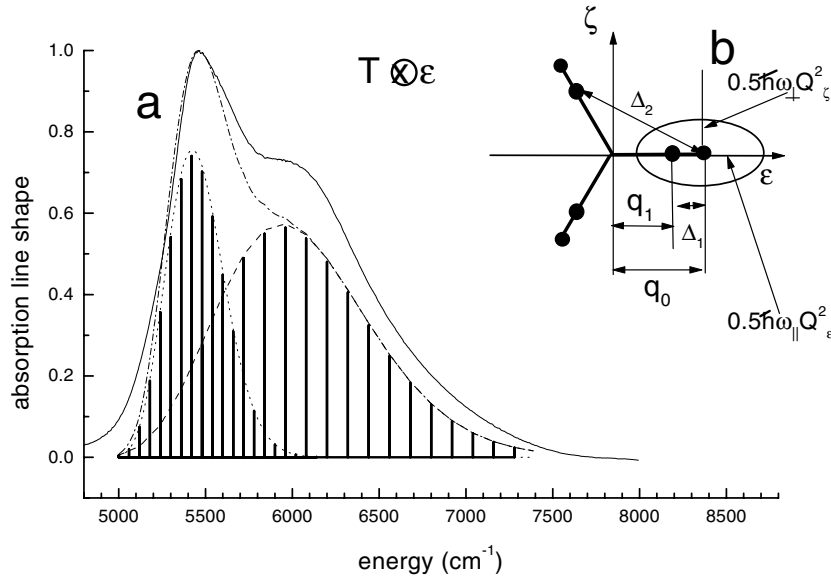
Figure 2. (a) The absorption line shape reproduced for the $^4T_1 \rightarrow {}^4T_2$ transition obtained under the assumption of the existence of the $T \otimes \varepsilon$ Jahn–Teller effect. Bands 1 and 2, which contribute to the spectrum, are represented by phonon lines as well as by the envelopes. The solid curve represents the experimental absorption line shape. (b) Positions of the energy minima of the ground and excited electronic manifolds in the two-dimensional configurational space. (q_0 and q_1 represent the ground and excited electronic manifolds, respectively.)

where Δ_1 and Δ_2 are the distances between the respective minima in the configurational space. Due to the degeneracy, the intensity of the second band is double the intensity of the first band. The line shape has been composed from vibronic overlap integrals as follows:

$$I(E) = \frac{1}{K} \sum_n |\langle \chi_{g1}^0 | \chi_{e1}^n \rangle|^2 \delta[E - (E_0 + n\hbar\omega_1^e)]$$

$$+ \frac{K-1}{K} \sum_n |\langle \chi_{g2}^0 | \chi_{e2}^n \rangle|^2 \delta[E - (E_0 + n\hbar\omega_2^e)] \tag{8}$$

where the coefficient related to the number of equivalent minima $K = 3$. $|\chi_{e1}^n\rangle$, $|\chi_{e2}^n\rangle$ and $|\chi_{g1}^0\rangle$, $|\chi_{g2}^0\rangle$ are the vibronic wave functions, which correspond to the effective vibronic modes in the first and second band, in the excited and ground states, respectively. The superscripts correspond to the excitation numbers; subscripts 1 and 2 correspond to the first and second band. The vibronic overlap integrals have been calculated using Manneback [18] recurrence formulae. The absorption line shapes reproduced are presented in figure 2(a). It is evident that to reproduce the band shape (especially the fact that the bandwidth of band 2 is broader), one needs different energies of phonons for the lower and upper bands. The phonon energies used in the calculations have been taken as the energies of the effective vibration modes that represent the vibrations in configurational coordinate space parallel to the vectors Δ_1 and Δ_2 for the bands 1 and 2, respectively. Thus for the band with lower energy (band 1), the energy of the effective phonon mode in the ground and excited state is $\hbar\omega_\parallel$. In form (8) one puts $\hbar\omega_1^e = \hbar\omega_\parallel$. For band 2, the energies of the effective phonon modes in the ground and excited electronic manifolds are given by

$$\hbar\omega_2^g = \hbar\omega_\parallel \sin^2 \alpha + \hbar\omega_\perp \cos^2 \alpha \tag{9}$$

and

$$\hbar\omega_2^e = \hbar\omega_\parallel \sin^2 \beta + \hbar\omega_\perp \cos^2 \beta \tag{10}$$

where

$$\alpha = \arccos\left(\frac{q_1^2 - q_0^2 - \Delta_2^2}{2q_0\Delta_2}\right)$$
$$\beta = \arccos\left(\frac{q_0^2 - q_1^2 - \Delta_2^2}{2q_1\Delta_2}\right). \tag{11}$$

To satisfy the condition that absorption band 2 is broader than band 1, we need to use a large value of the energy of the effective phonon modes that are responsible for the homogeneous broadening of band 2. Moreover, the energy of the effective mode in the excited electronic manifolds has to be greater than that in the ground electronic manifolds. Considering the adiabatic potentials given by relation (6), the above-mentioned conditions can be satisfied when $\hbar\omega_\parallel < \hbar\omega_\perp$ and under the assumption that the Jahn–Teller effect is much stronger in the ground state. The best fit that was obtained is presented in figure 2(a). We have used $E_0 = 5000$ cm^{-1}, $\frac{1}{2}\Delta_1^2 = 455$ cm^{-1}, $\frac{1}{2}\Delta_2^2 = 1055$ cm^{-1} which are fixed data resulting directly from the experimental absorption line shape. The other data that quantify the system are presented in table 1.

One can see that the calculated intensity of the second band is underestimated with respect to the experiment. This is why we consider the $T \otimes \tau$ Jahn–Teller coupling. The corresponding Hamiltonian is given as follows [16, 17]:

$$\frac{1}{2}Q_\xi^2 + \frac{1}{2}Q_\xi^2 + \frac{1}{2}Q_\eta^2 + V^{e,g} \begin{bmatrix} 0 & Q_\zeta & Q_\eta \\ Q_\zeta & 0 & Q_\xi \\ Q_\eta & Q_\xi & 0 \end{bmatrix}. \tag{12}$$

Table 1. Parameters of the configurational coordinate diagrams of the octahedrally coordinated Co^{2+} in the presence of T $\otimes$ ε and T $\otimes$ τ Jahn–Teller coupling.

	T $\otimes$ ε	T $\otimes$ τ
Jahn–Teller displacement in the ground state q_0 (relative units)	0.19	0.21
Jahn–Teller displacement in the excited state q_1 (relative units)	4.09	4.11
Jahn–Teller stabilization energy in the excited state (cm^{-1})	1.2	1.3
Jahn–Teller stabilization energy in the ground state (cm^{-1})	502	507
$\hbar\omega_\parallel$ (cm^{-1})	60	60
$\hbar\omega_\perp$ (cm^{-1})	120.1	120.1
Δ_1 (relative units)	3.90	3.90
Δ_2 (relative units)	4.19	4.19
$\hbar\omega_2^g$ (cm^{-1})	78	71
$\hbar\omega_2^e$ (cm^{-1})	120	120

As a result, the ^{4}T$_1$ state is split into four equivalent electronic manifolds with the minima of energy in the following positions [17] in $\{Q_\zeta, Q_\xi, Q_\eta\}$ space:

$$Q_1^{eg} = \frac{2}{3}V^{eg}\{q_\zeta, q_\xi, q_\eta\}$$

$$Q_2^{eg} = \frac{2}{3}V^{eg}\{q_\zeta, -q_\xi, -q_\eta\}$$

$$Q_3^{eg} = \frac{2}{3}V^{eg}\{-q_\zeta, -q_\xi, q_\eta\}$$

$$Q_4^{eg} = \frac{2}{3}V^{eg}\{-q_\zeta, q_\xi, -q_\eta\}.$$

(13)

The positions of the energy minima are presented in figure 3(b). As in the case of T $\otimes$ ε, we have assumed that the peaks of the absorption have energies given by relation (7). Also the absorption band shape has been calculated using the same method as in the case of T $\otimes$ ε coupling. Since the T $\otimes$ τ coupling needs three-dimensional coordinate space, the potential surfaces are given by the following relation:

$$U(Q) = \frac{1}{2}\hbar\omega_\parallel(Q_\parallel - Q_\parallel^0)^2 + \hbar\omega_\perp Q_\perp^2$$

(14)

where subscripts $\parallel$ and $\perp$ correspond to the vibration parallel and perpendicular to the Jahn–Teller displacement (the parallel-direction parameters are Q_1, Q_2, Q_3 or Q_4 (see (13)).

We have calculated the spectra using relations (8), (9), (10) and (11) assuming that the degeneracy coefficient for the T $\otimes$ τ system is $K = 4$. The best fit obtained is presented in figure 3(a). We have used the values $E_0 = 5000$ cm^{-1}, $\frac{1}{2}\Delta_1^2 = 455$ cm^{-1}, $\frac{1}{2}\Delta_2^2 = 1055$ cm^{-1}, as in the case of T $\otimes$ ε. The other data that quantify the system are presented in table 1. We have obtained an excellent fit of the theory to the experimental spectral line shape under the assumption of coupling to the three-dimensional τ-mode.

It should be noted that the existence of the strong Jahn–Teller distortion in the ground state influences the crystal-field calculations strongly. Usually, one assumes that the crystal-field strength is equal to the energy of the absorption spectrum peak (consider for instance the ^{4}A$_2 \rightarrow$ ^{4}T$_2$ transition in the octahedrally coordinated Cr^{3+} system [12]). In this case the ground
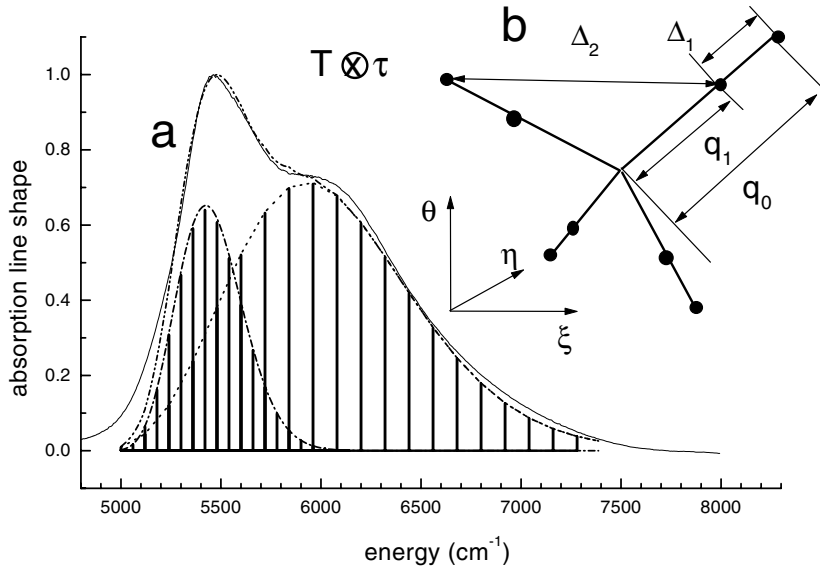
Figure 3. (a) The absorption line shape reproduced for the $^4T_1 \rightarrow \, ^4T_2$ transition obtained under the assumption of the existence of the $T \otimes \tau$ Jahn–Teller effect. Bands 1 and 2, which contribute to the spectrum, are represented by phonon lines as well as by the envelopes. The solid curve represents the experimental absorption line shape. (b) Positions of the energy minima of the ground and excited electronic manifolds in the three-dimensional configurational space. (q_0 and q_1 represent the ground and excited electronic manifolds, respectively.)

state is the symmetric orbital singlet, $^4A_2$; thus even if lattice relaxation in the ground state takes place, the ion displacements are symmetrical and do not introduce a lower-symmetry crystal field. Since the electron–lattice coupling in the ground state creates only a cubic crystal field, the positions of the ions that correspond to the minimum energy of the ground electronic manifold can be used for determining $10Dq$, independently of whether the relaxation of the system in the ground state takes place or not. Thus the value of $10Dq$ which is equal to the energy corresponding to the $^4A_2 \rightarrow \, ^4T_2$ absorption line shape is accurate. Specifically, one can use such values for accurate prediction of the energies of other excited states of the Cr^{3+} system. In this case, one can calculate the crystal-field strength and lattice relaxation energy separately.

If the ground state is split by the Jahn–Teller effect, the shifts of the ions in the ground state result in unsymmetrical distortion. Since the field that is created is not cubic, the lattice relaxation, although it influences the energy of the minima of the ground and excited electronic manifolds, does not change the crystal-field parameter $10Dq$. As a result, the $^4T_1 \rightarrow \, ^4T_2$ absorption maximum appears for energy greater than the value of $10Dq$. To obtain the actual values of $10Dq$ from the absorption spectrum, one has to relate them to the unrelaxed lattice. Our analysis of the Jahn–Teller effect is presented in figure 4. One calculates the separation energy that corresponds to the unrelaxed lattice from the energy of the zero-phonon line and the Jahn–Teller stabilization energies in the ground and excited states:

$$10Dq = E_0 + E_{JT}(\text{g}) - E_{JT}(\text{e}). \tag{15}$$

The value $10Dq = 4750$ cm^{-1} obtained in this way is smaller than the zero-phonon energy, E_0, and smaller than the energies of the absorption bands.
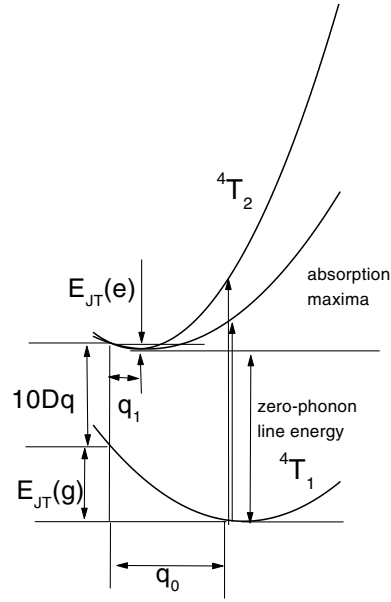
Figure 4. A configurational coordinate diagram that represents the cross-section through the $\{Q_\zeta, Q_\xi, Q_\eta\}$ space in the $\{1, 1, 1\}$ direction. In the diagram, only one electronic manifold representing the ground ^{4}T$_1$ state and two electronic manifolds that represent the first excited ^{4}T$_2$ states are presented.

4. Conclusions

Analysis of the absorption spectrum of Co-doped SrLaGa$_3$O$_7$ in the framework of the crystal-field approach allows us to conclude that we are dealing with octahedrally coordinated Co^{2+} ions, which replace Sr^{2+} in the lattice. The detailed analysis of the absorption band shape shows the existence of the T $\otimes$ τ Jahn–Teller effect in the ground ^{4}T$_1$ state. Actually, one can exclude the possibility that the structure of the ^{2}T$_1$ $\rightarrow$ ^{4}T$_2$ absorption band is related to the ^{4}T$_2$-state splitting induced by the lower-symmetry field. In the octahedrally coordinated system the initial symmetry O$_h$ can be reduced to D$_4$, D$_3$, C$_4$, C$_3$ and C$_2$ symmetries. The first two cases would result in splitting of the T$_2$ state into B$_2$ and E, and A$_1$ and E states respectively. Since A$_1$ and B$_2$ are not degenerate and E is doubly degenerate, one expects the intensity ratio of the absorption bands to be equal to 1:2. We have shown that when the analysis of the static T $\otimes$ ε Jahn–Teller effect has been considered, this is not correct. The lowering of the symmetry to C$_4$, C$_3$ or C$_2$ would cause the splitting of the T$_2$ state into three non-degenerate levels. If the ^{4}T$_1$ $\rightarrow$ ^{4}T$_2$ absorption is considered, this is also not the case here. The actual intensity ratio of band 2 to band 1 is equal to 3:1, which strongly supports the existence of a T $\otimes$ τ Jahn–Teller effect that splits the ^{4}T$_2$ as well as the ^{4}T$_1$ state into four equivalent electronic manifolds.

One should note the non-linearity of the system that is manifested by the different effective phonon energies for the parallel and perpendicular vibrations. Although we have not performed detailed calculations, we argue that this effect is typically dynamic and is related to the processes of tunnelling between the Jahn–Teller-split electronic manifolds, induced by the spin–orbit interaction. As long as the zero-phonon states are considered, the spin–orbit coupling yields a smoothing of the adiabatic potential curvature near the bottom of the hypersurfaces. This

is why, for both effective modes, the phonon energies in the ground state are small and independent of the direction in the configuration space ($\hbar\omega_2^{\mathrm{g}} \cong \hbar\omega_\parallel$). For the higher vibronic energies, the spin–orbit interaction influences the potential curvature only in the directions where the hypersurfaces cross. This is why in the excited state the energies of the effective modes are different ($\hbar\omega_2^{\mathrm{e}} \gg \hbar\omega_\parallel$) for different modes.

Acknowledgment

References

[1] Berkowski M, Borowiec M, Pataj K, Piekarczyk W and Wardzyński W 1984 *Physica* B + C **123** 215–9
[2] Kaminskii A A, Belokoneva E L, Mill B V, Sarkisov S E and Kurbanov K 1986 *Phys. Status Solidi* a **97** 279–90
[3] Ryba-Romanowski W, Gołąb S, Dominiak-Dzik G, and Berkowski M 1992 *Mater. Sci. Eng.* B **15** 217–21
[4] Pracka I, Giersz W, Świrkowicz M, Pajączkowska A, Kaczmarek S M, Mierczyk Z and Kopczyński K 1994 *Mater. Sci. Eng.* B **26** 201–6
[5] Kaczmarek S M, Mierczyk Z, Kopczyński K, Frukacz Z, Pracka I and Łukasiewicz T 1995 *Proc. SPIE* **2772** 139–42
[6] Kaczmarek S M, Berkowski M and Jabłoński R 1999 *Cryst. Res. Technol.* **34** 1023–9
[7] Kubota S, Izumi M, Yamane H and Shimada M 1999 *J. Alloys Compounds* **283** 95–100
[8] Malinowski, M, Pracka I, Myziak P, Piramidowicz R and Wolinski W 1997 *J. Lumin.* **72–74** 224–5
[9] Simondi-Teisseire B, Viana B, Lejus A M and Vivien D 1997 *J. Lumin.* **72–74** 971–3
[10] Abragam A and Bleaney B 1970 *Electron Paramagnetic Resonance of Transition Ions* (Oxford: Clarendon)
[11] Ferguson J, Wood D L and Knox K 1963 *J. Chem. Phys.* **39** 881–9
[12] Henderson B and Imbusch G F 1989 *Optical Spectroscopy of Inorganic Solids* (Oxford: Oxford University Press)
[13] Sugano S, Tanabe Y and Kamimura H 1970 *Multiplets of Transition Metal Ions in Crystal* (New York: Academic)
[14] Tsuboi T and Iio K 1990 *Phys. Rev.* B **41** 4770–3
[15] Macfarlane R M, Wong J Y and Sturge M D 1968 *Phys. Rev.* **166** 250–8
[16] Englman R 1972 *The Jahn–Teller Effect in Molecules and Crystals* (London: Wiley–Interscience)
[17] Ghelichkhani E and Grant E R 1991 *Chem. Phys. Lett.* **187** 309–16
[18] Manneback C 1951 *Physica* **17** 1001–10

Annotations from 16105sm.pdf

Page 2

Annotation 1; Label: Author:; Date: 02/01/2001 12:35:55
Amended wording of this sentence OK?

Page 3

Annotation 1; Label: Author:; Date: 02/01/2001 12:36:21
Amended wording of this sentence OK?

Page 4

Annotation 1; Label: Author:; Date: 02/01/2001 12:36:42
Amended wording `We will now' OK?

Page 5

Annotation 1; Label: Author:; Date: 02/01/2001 12:37:00
Amended wording `assume' OK?

Page 6

Annotation 1; Label: Author:; Date: 02/01/2001 12:37:28
Amended wording `which are' OK?

Annotation 2; Label: Author:; Date: 02/01/2001 12:37:50
Should the first subscript be zeta?

Page 7

Annotation 1; Label: Author:; Date: 02/01/2001 12:38:10
Amended wording `parameters' OK?

Page 8

Annotation 1; Label: Author:; Date: 02/01/2001 12:38:47
Amended wording `which is' and `is accurate' OK?

Page 9

Annotation 1; Label: Author:; Date: 02/01/2001 12:39:08
Amended wording `possibility' OK?

Annotation 2; Label: Author:; Date: 02/01/2001 12:39:28
Amended wording of this sentence OK?